97 - 42

A.N.Akimov[1], L.A.Vlasukova[1], G.A.Gusakov[1], F.F.Komarov[1],
M.Kulik[2], A.Latuszyński[2], D.Mączka

STRUCTURE-PHASE TRANSFORMATION
UNDER ION IMPLANTATION INTO GaAs

[1]Belarussian State University, Minsk, Republik of Belarus
[2]Institute of Physics, Marie Curie-Skłodowska University, Lublin, Poland

1997

Introduction

Among $A^{III} B^{V}$ compounds the gallium arsenide is the material in which the processes of radiation damage formation and annealing during the ion implantation have the essential influence on the structure of the implanted layer [1, 2]. In whole for $A^{III} B^{V}$ compounds the influence of implantation parameters on the structure of implanted layer is essentially more than for elementary semiconductors. This difference is connected with the complication of physical processes taking place in irradiating binary semiconductors. It is necessary to take into account that the conditions for transformation and annealing during the implantation of primary radiation damage are less hard in ion-covalent $A^{III} B^{V}$ crystals as compared with covalent Si [3]. In result at, the same dose the variation of other implantation parameters (energy of implanting ions, beam current density and so on) leads to formation of implanted layers which differ by the types, concentration and location of damage. It is known that the nature of damage in irradiated crystals defines peculiarities and degree of the structure restoration during the postimplantation thermal treatment. More over the effect, of high dose observing for GaAs [4, 5] is more complicated than one for elementary semiconductors. So, it is necessary to analyse in detail the dependence of the processes of defects formation and amorphization in GaAs on the parameters of implantation for explanation of the disorder evolution and the final properties of implanted layer.

In the present paper the processes of structure disordering in GaAs implanted by 100 keV Ar^+ and P^+ ions with different beam current densities have been investigated by the methods of Raman spectroscopy (RS), of He^+ ions channelling and transmission electron microscopy (TEM). It was shown in [6,7] that, the process of crystals disordering carried the nonmonotonous, oscillating character with dose especially for binary semiconductors. So the main aim of the work is the definition of beam current density and dose intervals of nonmonotonous changes of the structure perfection.

Experiment

Single-crystal, <100> - oriented GaAs with resistivity $\rho > 10^7$ Ohm·cm was used as the starting material. The samples were implanted with 100 keV P^+ and Ar^+ ions in the dose range from $6 \cdot 10^{12}$ to $5 \cdot 10^{16}$ cm^{-2}. The implantation of P^+ ions was carried out at current densities j of 0,1 and 1 $\mu A/cm^2$. The current densities for Ar^+ implantation were 1 and 2,5 $\mu A/cm^2$. The samples for each series were prepared from the same plate. The implantation was carried out using UNIMAS implanted under the target thermal insulating conditions [8]. Raman spectra were obtained in backscattered geometry with U-1000 (Jobin-Yvon) spectrometer under Ar-laser excitation (t = 514,5nm). The samples were analysed with 1,5 MeV He^+ Rutherford backscattering (RBS) in

combination with the channelling. The backscattered particles were detected at a scattering angle of 170°. RBS spectra were obtained using a high Voltage 2 MeV accelerator. Selected samples of P^+ implanted GaAs were analysed with TEM in plan-view technique.

Using of RS allows to observe simultaneously the sharp intensive peak of crystalline phase and the diffusive band of amorphous phase that gives the possibility to investigate the dynamics of phase transitions in the subsurface layer. The depth distribution of damage and the kinetics of structure transformation in the volume of implanted layer can be studied with the RBS channelling technique. The TEM data give information about the nature of damage in the implanted layer.

Results and Discussion

The RS spectra of initial sample of GaAs and samples implanted with different dose of Ar^+ ions at current density j = 1 $\mu A/cm^2$ are presented in Fig. 1a. In spectra of implanted samples the increasing of dose leads to decreasing of allowing for <100> orientation LO-phonon peak intensity and displacement of its maximum to the side of low frequencies. At the same time the intensity of forbidden for this orientation TO-phonon peak increases with dose. The relationship between the intensities of forbidden TO-phonon and allowed LO-phonon peaks I_{TO}/I_{LO} can be used for the estimation of the disorder degree of crystals. Value of I_{TO}/I_{LO} for GaAs samples implanted with Ar^+ ions at j - 1 $\mu A/cm^2$ are presented in Tab. 1. It follows from Tab.1 that I_{TO}/I_{LO} relationship decreases monotonously with dose. Moreover the increasing of dose leads to formation in RS spectra of the broad bands in the range of (150-200) cm^1 and (200-300) cm^1 which correspond to amorphous GaAs. For D - 1 $\mu A/cm^2$ the LO-phonon peak is still displayed in RS spectrum on the background of (200-300) cm^1 band. The further increasing of dose leads to disappearance of the crystalline GaAs peaks from RS spectra. The entirely different picture is observed for the samples implanted with Ar^+ ions at j - 2,5 $\mu A/cm^2$ (Fig.1b).
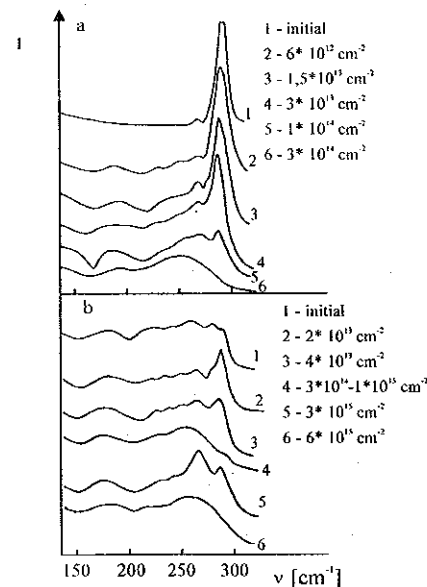

Figure 1. RS spectra (λ=514,5 nm) obtained from GaAs samples implanted with 100 keV Ar^+ ions at current densities: a-1 $\mu A/cm^2$; b-2,5 $\mu A/cm^2$.

a
1 - initial
2 - $6* 10^{12}$ cm^{-2}
3 - $1,5*10^{13}$ cm^{-2}
4 - $3* 10^{13}$ cm^{-2}
5 - $1* 10^{14}$ cm^{-2}
6 - $3* 10^{14}$ cm^{-2}

b
1 - initial
2 - $2* 10^{13}$ cm^{-2}
3 - $4* 10^{13}$ cm^{-2}
4 - $3*10^{14}$-$1*10^{15}$ cm^{-2}
5 - $3* 10^{15}$ cm^{-2}
6 - $6* 10^{15}$ cm^{-2}

150 200 250 300 ν [cm^{-1}]

Dose [cm^{-2}]	v_c of LO-phonon peak [cm^{-1}]	v_c of TO-phonon peak [cm^{-1}]	I_{TO}/I_{LO}	Γ_c of LO-phonon peak [cm^{-1}]
E = 100 keV, j = 1 μA/cm^2				
$6*10^{12}$	291	267	0,20	6,9
$1,5*10^{13}$	289	267	0,37	9,7
$3*10^{13}$	287	266	0,52	12,4
$1*10^{14}$	287	268	0,82	18,1
$3*10^{14}-6*10^{15}$	-	-	-	-
E = 100 keV, j = 2,5 μA/cm^2				
$2*10^{13}$	283	-	-	22,1
$4*10^{13}$	289	266	0,52	11,1
$1*10^{14}$	288	267	1,00	15,2
$3*10^{14}$	-	-	-	-
$6*10^{14}$	-	-	-	-
$1*10^{15}$	-	-	-	-
$3*10^{15}$	288	267	1,33	13,9
$6*10^{15}$	-	-	-	-
Initial sample				
-	293	266	0,05	5,6

Table 1. Spectral characteristics of GaAs samples implanted with Ar$^+$ ions.

For D = $2*10^{13}$ cm^2 the RS spectrum is characterised by "amorphous" bands at 150-200 cm^{-1} and 200-300 cm^{-1}. The LO-phonon peak exists as a faint maximum at 283 cm^{-1}. The further increasing of dose leads to nonmonotonous changes in RS spectra. The LO- and TO-phonon peaks of crystalline GaAs are observed for samples implanted with doses $4*10^{13}$, $1*10^{14}$ and $3*10^{15}$ cm^{-2}. Spectra of samples implanted with doses $3*10^{14}$, $6*10^{14}$, $1*10^{15}$ and $6*10^{15}$ cm^{-2} are characterised by "amorphous" bands at (150-200) cm^{-1} and (200-300) cm^{-1}.

The same changes in RS spectra of GaAs implanted with Ar$^+$ ions in the dose range $6*10^{12}$ - $1,2*10^{15}$ cm^{-2} was observed in [6]. Oscillating character of the structure perfection changes taken place in the dose range $1*10^{14}$ - $1,2*10^{15}$ cm^{-2} when the energy of implanting ions E $\geq$ 150 keV. Unfortunately the absence in [6] of information about the current density makes difficult the detail comparison of the obtained results.

Figure 2a shows the dose dependence of the frequency location v_c and the width on the half of maximum height Γ_c of the LO-phonon peak of crystalline GaAs for the Ar$^+$ implantation at j = 1 and 2,5 μA/cm^2. It follows from figure that for j = 1 μA/cm^2 the value of Γ_c increases monotonously with dose. The maximum value of Γ_c equated to 18,1 cm^{-1} being obtained at D = $1*10^{14}$ cm^{-2}.
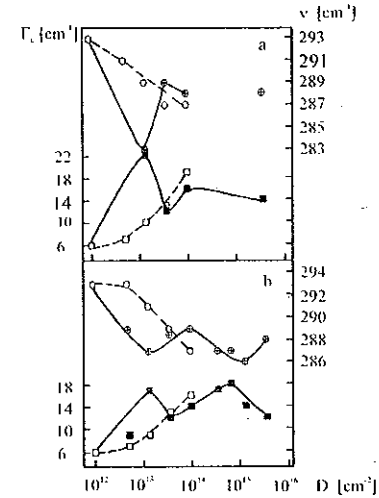
Figure 2. The dose dependence of the frequency location and the width on the half of maximum height of the LO-phonon peak; a - for Ar$^+$ implanted samples at j = μA/cm^2 (dashed lines) and at j = 2,5μA/cm^2 (solid lines); b - for P$^+$ implanted samples at j = 0,1μA/cm^2 (dashed lines) and at j = 1μA/cm^2 (solid lines).
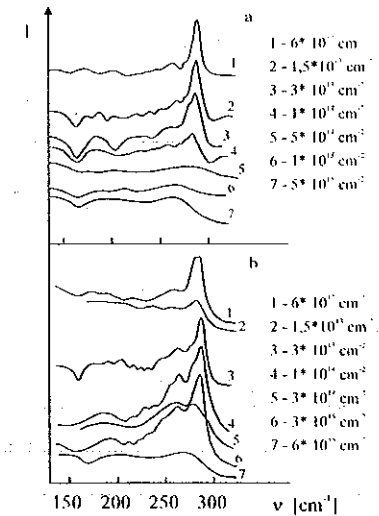
Figure 3. RS spectra (1 = 514,5 nm) obtained from GaAs implanted with 100 keV P$^+$ ions at current densities: a - j = 0,1 μA/cm^2; b - j = 1 μA/cm^2.

The value of v_c decreases with dose till 287 cm^{-1} (D - $1*10^{14}$ cm^{-2}). The further increasing of dose leads to disappearance of LO-phonon peak in RS spectra. For j = 2,5 μA/cm^2 the value of Γ_c changes nonmonotonously with dose. It follows from fig. 2a that the dependence of v_c from dose has two minima at D of $4*10^{13}$ and $3*10^{15}$cm^{-2}.

The observing decreasing of v_c could be connected with increasing of the average microcrystallites size (model of phonons spatial correlation [9]) and/or with the ion-induced annealing of radiation damage [5]. The changes of v_c correlate with the changes of v_c.

RS spectra of GaAs implanted with P$^+$ ions are adduced in Fig. 3 and the corresponding spectral characteristics are presented in Tab. 2. For j = 0,1 μA/cm^2 (Fig. 3a) the intensity of LO-phonon peak decreases with dose and its maximum displaces to the side of low frequencies as for case of Ar$^+$ ions implantation at j = 1 μA/cm^2. The broad bands of amorphous GaAs appears at (150-200) and (200-300) cm^{-1} at dose of $1,5*10^{13}$ cm^{-2}. Their intensity increases with dose and at D = $5*10^{14}$ cm^{-2} the samples are characterised only by amorphous bands. For j = 1 μA/cm^2 (Fig. 3b) the nonmonotonously character of the RS spectra transformation with dose is observed. The amorphous bands appear in spectra already at

dose of $6 \cdot 10^{12}$ cm^{-2}. The further increasing of dose leads to nonmonotonous changes in RS spectra. The LO- and TO-phonon peaks of crystalline GaAs are observed for samples implanted with doses $3 \cdot 10^{13}$, $1 \cdot 10^{14}$, $6 \cdot 10^{14}$, $1 \cdot 10^{14}$, and $3 \cdot 10^{15}$ cm^{-2}. Spectra of samples implanted with doses $1,5 \cdot 10^{13}$, $3 \cdot 10^{14}$, and $6 \cdot 10^{15}$ cm^{-2} are characterised by amorphous bands at (150-200) cm^{-1} and (200-300) cm^{-1}.

Dose [cm^{-2}]	ν_c of LO-phonon peak [cm^{-1}]	ν_c of TO-phonon peak [cm^{-1}]	I_{TO}/I_{LO}	Γ_c of LO-phonon peak [cm^{-1}]
E = 100 keV, j = 0, 1 μA/cm^2				
$6 \cdot 10^{12}$	293	265	0,25	6,9
$1,5 \cdot 10^{13}$	291	268	0,35	9,7
$3 \cdot 10^{13}$	289	-	-	12,5
$1 \cdot 10^{14}$	287	-	-	15,3
$5 \cdot 10^{14}$-$5 \cdot 10^{15}$	-	-	-	-
E = 100 keV, j = 1 μA/cm^2				
$6 \cdot 10^{12}$	289	260	0,27	9,7
$1,5 \cdot 10^{13}$	287	-	-	16,7
$3 \cdot 10^{13}$	289	267	0,51	12,5
$1 \cdot 10^{14}$	289	268	0,68	13,9
$3 \cdot 10^{14}$	287	-	-	16,7
$6 \cdot 10^{14}$	287	269	1,24	18,1
$1 \cdot 10^{15}$	286	278	0,96	13,9
$3 \cdot 10^{15}$	288	266	0,62	11,8
$6 \cdot 10^{15}$	-	-	-	-
Initial sample				
-	293	266	0,05	5,6

Table 2. Spectral characteristics of GaAs samples implanted with P$^+$ ions.

Figure 2b shows the dose dependence of the frequency location ν_c and the width on the half of maximum height Γ_c of the LO-phonon peak of crystalline GaAs for the P$^+$ ion implantation at j = 0,1 and 1 μA/cm^2. It follows from the figure that for j = 0,1 μA/cm^2 the value of Γ_c increases monotonously with dose. The maximum value of Γ_c equated to 15, 3 cm^{-1} being obtained at D = $1 \cdot 10^{14}$ cm^{-2}. The further increasing of dose leads to disappearance of LO-phonon peak in RS spectra. For j = 1 μA/cm^2 the changes of Γ_c and ν_c with dose have an oscillating character. It follows from Fig. 2b that the dependence of from dose has two maxima at D of $1,5 \cdot 10^{13}$ and $6 \cdot 10^{14}$ cm^{-2}. The same nonmonotonous changes are observed for ν_c.

The dose dependence of spectral characteristics for P$^+$ implanted GaAs at j = 1 μA/cm^2 is similar to one for the Ar$^+$ implantation at j = 2,5 μA/cm^2. But the value of Γ_c and the changes of Γ_c and ν_c for P$^+$ implantation are smaller that one for Ar$^+$ implantation. The comparison of Γ_c and ν_c changes shows that P$^+$ implantation in the self - annealing regimes is characterised by lower disordering of the irradiated layer.
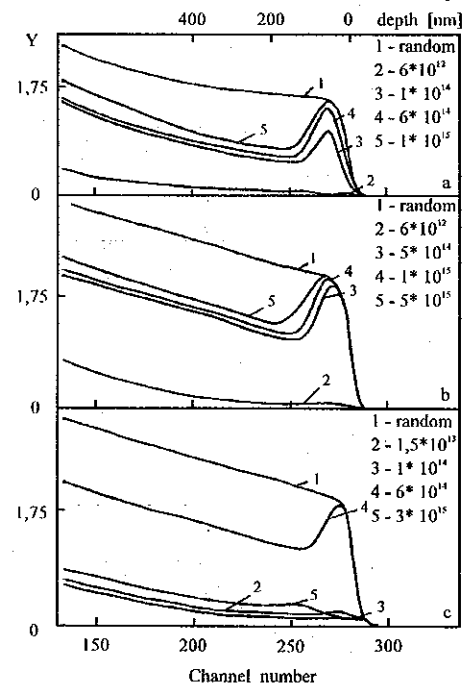

Figure 4. RBS/channelling spectra of He$^+$ ions with E=1,5 MeV from GaAs samples implanted with: a - Ar$^+$ ions at j=1μA/cm^2; b - P$^+$ ions at j=μA/cm^2; c - P$^+$ ions at j=1μA/cm^2.

The RBS spectra for Ar$^+$ implanted GaAs at j = 1 μA/cm^2 are presented in Fig. 4a. For the low doses the disorder degree is small. At D = $1 \cdot 10^{14}$ cm^{-2} the distinct damage peak appears on the depth of ~ 50 nm that corresponds to estimated value of R_{pD} (routine TRIM88). The further increasing of dose leads to damage increasing and formation of the extended amorphous layer at D = $1 \cdot 10^{15}$ cm^{-2}.

The RBS data for P$^+$ implantation at j = 0,1 μA/cm^2 (Fig. 4b) show the monotonous increasing of disorder degree with dose. The amorphous layer forms at D = $5 \cdot 10^{14}$ cm^{-2}. At dose of $5 \cdot 10^{15}$ cm-2 the thickness of the amorphous layers about 150 nm.

For the P$^+$ implantation at j = 1 μA/cm^2 (Fig. 4c) the disorder degree increase right up to dose of $6 \cdot 10^{14}$ cm^{-2}. But the further increasing of dose leads to considerable damage annealing. The RBS data for D = $3 \cdot 10^{15}$ cm^{-2} indicate almost complete restoration of crystalline structure in the ~ 80 nm thick surface layer. The increasing of yield of the backscattering ions from the depth > R_p (R_p ~ 84 nm) witnesses about the formation of secondary extended defects in region between R_p and $2R_p$.

For more detailed analysis of the structure-phase transformations observing in GaAs implanted with P$^+$ ions at j = 1 μA/cm^2 the TEM investigations in plan-view technique have carried out. From the RS data follow that the first crystal-amorphous state-crystal phase transition takes place in the dose interval of $6 \cdot 10^{12}$ - $3 \cdot 10^{13}$ cm^{-2}. For doses of $6 \cdot 10^{12}$ and $3 \cdot 10^{13}$ cm^{-2} the samples can

be characterised as the crystals with defects. But the TEM shows the presence on the surface of thin amorphous layer for the sample implanted with dose of $1,5 \cdot 10^{13}$ cm^{-2}. Obtained results are in a good agreement with the RS data.

The second dose interval of phase transition is between $1 \cdot 10^{15}$ and $6 \cdot 10^{16}$ cm^{-2}. For $D = 1 \cdot 10^{15}$ cm^{-2} the diffraction pattern (Fig. 5a) shows the presence on the surface of amorphous layer with thickness less than 60 nm. The sample implanted with dose of $3 \cdot 10^{16}$ cm^{-2} is characterised by the disordered crystalline structure with the dislocation loops (Fig. 5b). The density of dislocation loops is in interval from 10^{10} to 10^{12} cm^{-2}.
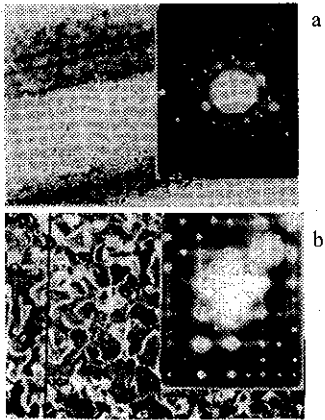
Figure 5. Plan-view image (left) and diffraction pattern (right) of GaAs samples implanted with P$^+$ ions: a - D = $1 \cdot 10^{15}$cm^{-2}; b -D = $3 \cdot 10^{15}$cm^{-2}.

Figure 6. Plan-view image (left) and diffraction pattern (right) of GaAs samples implanted with P$^+$ ions at D = $6 \cdot 10^{15}$cm^{-2}; a - amorphous region; b - polycrystalline region; c - crystal with microtwins.

It follows from the TEM data that the damaged layer of the sample implanted with dose of $6 \cdot 10^{15}$ cm^{-2} has the most complicated structure and consists of several regions with the different disorder degree. In the plan-view technique scanning of the analysing electron beam along the wedgelike edge of the hole which being formed in the investigated sample by the chemical etching allows to obtain the diffraction patterns from the layers of different thickness. In this way one can observe the structure of the damaged layer. The obtained diffraction patterns fix the presence of the sufficiently thick amorphous layer (Fig. 6a), the polycrystalline phase (Fig. 6b) and microtwins

oriented in <111> - direction (Fig. 6c). The plan-view technique does not allow to value the depth distribution of defects. So, it is necessary the additional TEM investigation in cross-section technique to obtain the information about thickness and location of the regions with the different disorder degree.

The discrepancy between RS and TEM data for the samples implanted with D = $6 \cdot 10^{15}$ cm^{-2} is connected with the decreasing of depth of RS-testing layer under its amorphization. Depth of RS-testing layer d is determined by the absorption coefficient of substance. At $\lambda = 514,5$ nm d is equal to 110 and 30 nm for crystalline and amorphous GaAs, accordingly [6]. Therefore, the presence of amorphous layer in the surface region leads to decreasing of testing depth d to 30 nm. In the first dose interval of the phase transition the processes of structure transformation take place in the thin surface layer testing with RS. In the second dose interval the surface amorphous layer prevents to analyse the phase transition processes occurring at the more deep region of implanting layer.

Summary and Conclusions

The dependence of ion-beam-induced crystallisation and amorphization of GaAs on dose rate and type of implanting ions has been investigated with Rutherford backscattering, Raman spectroscopy and transmission electron microscopy techniques. The results can be summarised by the following conclusions:

1. At the low ion beam current, density the disorder degree increases monotonously with dose right, up to formation of the extended amorphous layer. The further increasing of dose leads to expansion of amorphous layer away from the surface.

2. If the ion beam current density is more than some critical value the dose dependence of the disorder degree has nonmonotonous character. We observed two cycles of the amorphous state - crystal - amorphous state transitions in dose interval from $6 \cdot 10^{12}$ to $6 \cdot 10^{15}$ cm^{-2}. The first phase transition takes place in interval of $6 \cdot 10^{12}$ - $3 \cdot 10^{13}$ cm^{-2}. Comparison of data obtained with different methods of analysis shows that the phase transformations occur only in thin surface layer (~ 30 nm-thickness). The further increasing of dose leads to formation of damage peak at depth $\sim R_{p0}$. The second phase transition occurs in dose interval of $5 \cdot 10^{14}$ - $6 \cdot 10^{15}$ cm^{-2}. The RBS, RS and TEM data show the presence in samples implanted with dose of $6 \cdot 10^{14}$ and $1 \cdot 10^{15}$ cm^{-2} of the extended amorphous layer. At dose of $3 \cdot 10^{15}$ cm^{-2} the almost complete restoration of the surface layer to depth $\sim$ Rp occurs. But the layer with high concentration of dislocation loops being formed region between R_p and $2R_p$. Finally, at the largest investigated dose of $6 \cdot 10^{15}$ cm^{-2} the samples have the most, complicated structure. TEM shows the presence in implanted layer of several regions with the different disorder degree.

3. Value of the critical in beam current, density depends on the type of implanting ions. The critical current density for elements of group V (P^+) is considerable less than for noble gases (Ar^+).

4. The second phase transition can be explained on the base of model of the ion-induced annealing. At the critical current density because of target heating by the ion beam the conditions when the rate of defect complexes formation is equal to the rate of their dynamic annealing can be realised. If the beam current density is more than critical value target heating leads to the prevalence of the annealing processes. But nature of the first phase transition and the dependence of the critical ion beam current density on the type of implanting ions is not clear. So, further studies are necessary to understand these ion-irradiation effects in GaAs.

Acknowledgements

References

1) E. Wendler, W. Wesch and G. Gotz, Nucl. Instr. Meth. B52, 789 (1991).

2) C. Ridgway, S. T. Johnson and R. G. Elliman, Nucl. Instr. Meth. B59/60, 454 (1991).

3) S. Vavilov and I. S. Tashlykov, Ionno-implantatsionnoe legirovanie arsenida galliya. Obzor po elektronnoy technike, ser. 2 Eletronnye pribory, N2 (1991).

4) Yu. A. Bumai, D. S. Domanevski, F. F. Komarov, A. P. Novikov, V. I. Hitko, A. G. Ulyashin, Rad. Eff. Express 1, 101 (1987).

5) A. N. Akimov, L. A. Vlasukova, G. A. Gusakov, F. F. Komarov, A. A. Kutas, A. P. Novikov, Rad. Eff. 129, 147 (1994).

6) V. Artamonov, M. Ya. Valah, V. L. Gromashevski, V. D. Nechiporchuk, V. V. Strelchuk, V. A. Uhimchuk, Fizika i Technika Poluprovodnikov 26, 725 (1992).

7) P.V. Zukovski, Fizika i Technika Poluprovodnikov 27, 789 (1993).

8) D. Maczka, A. Latuszynski, R. Kuduk, J. Partyka, Nucl. Instr. Meth. B21, 521 (1987).

9) K. Tiong, P. M. Amirtharai, F. N. Pollak, D. E. Aspnes, Appl. Phys. Lett. 44, 122 (1984).